EPiC Series in Built Environment
Volume 7, 2026, Pages 1182–1191
Proceedings of Associated Schools of Construction 62nd Annual International Conference

Prediction of Construction Workers' Thermo-Physiological Responses under Extreme Heat Stress

Md. Tushar Ali [1], Mohammad Khalid [1]
[1] New Jersey Institute of Technology

Monitoring construction workers' thermo-physiological responses, such as heart rate (HR), core temperature (T_{core}), and skin temperature (T_{skin}), is critical for managing heat stress (HS) under extreme environmental conditions. Continuous physiological monitoring is often impractical on construction sites due to workforce size, task variability, and differences in metabolic rate (MR) and individual characteristics. To address this gap, this study applies a modeling-based approach to simulate and predict hourly T_{core}, T_{skin}, and HR using modified Multi-Node Fiala Thermophysiological (MN-FTM) and Two-Node Thermo-Physiological (TN-TPM) models driven by meteorological and worker-specific inputs. Six simulation scenarios were developed to represent variations in worker attributes and heat exposure conditions. Results show pronounced physiological responses to HS, with peak strain occurring between 11:00 AM and 1:00 PM. HR and T_{core} exhibited strong nonlinear relationships across scenarios, while older and heavier workers demonstrated slower recovery during late-afternoon periods, and higher MR was associated with elevated T_{core}. The findings highlight the importance of identifying construction workers' thermophysiological risk factors to support targeted heat mitigation strategies. The presented computational framework can complement continuous field monitoring and be integrated into decision-support, safety-analytics, and training platforms, enhancing practitioners' capacity to apply simulation-based and data-informed heat-risk management.

Keywords: Heat Stress, Metabolic Rate, Core Temperature, Skin Temperature, Heart Rate, Construction Worker.

Introduction

The U.S. construction industry is one of the nation's largest economic sectors, employing nearly 8 million workers (Bureau of Labor Statistics 2025). Due to the physically demanding and predominantly outdoor nature of construction work, employees are routinely exposed to extreme HS. Particularly during summer or in hot and humid regions, construction workers are 13 times more likely to experience heat-related illness (HRI) than workers in other industries (Acharya et al. 2018). Skilled trade workers are especially vulnerable, as prolonged labor under direct sunlight increases fluid loss and core body temperature, leading to dehydration, fatigue, heat exhaustion, impaired alertness, and, in severe cases, heat stroke. Heavy personal protective equipment (PPE) and limited access to shade or ventilation further intensify thermal strain. Consequently, the construction sector continues to report high injury and illness rates, with 2.3 total recordable cases per 100 workers in 2023, including 1.5 cases involving days away from work or restricted duty (Bureau of Labor

Statistics 2025). Despite these risks, traditional heat assessment approaches still rely largely on environmental measures such as air temperature or Wet-Bulb Globe Temperature (WBGT), which do not account for individual variability related to age, body composition, workload, clothing insulation, or metabolic rate (Acharya et al. 2018).

This limitation is critical because HS is fundamentally driven by the balance between internal heat production and heat dissipation. In physically active workers, metabolic heat generated by muscle activity elevates T_{core}, while T_{skin} reflects the body's capacity to lose heat through convection, radiation, and evaporation (Cramer et al. 2022). Cardiovascular strain, typically measured via HR, increases as blood is redirected to the skin to support cooling mechanisms (Yermakova et al. 2022). Construction workers performing physically demanding tasks outdoors face a particularly high risk due to a combination of elevated metabolic heat, environmental exposure, and heavy PPE (Amorim and Schlader 2024). Empirical studies have shown substantial HS in these workers, with T_{core} exceeding 38.0 °C in nearly half of the participants during summer work, accompanied by elevated HR, indicating high physiological stress (Yermakova et al. 2022). Moreover, environmental factors such as air temperature, humidity, wind speed, solar radiation, and mean radiant temperature, along with clothing insulation, strongly influence heat dissipation (Amorim and Schlader 2024). Individual characteristics, including age, gender, body mass, and acclimatization, further modulate T_{core} and T_{skin} responses, demonstrating the limitations of generalized indices like the WBGT for predicting personal heat strain.

Recent studies have explored wearable and mobile sensing technologies to assess workers' physiological responses under simulated and field conditions. Buller et al. (2018) demonstrated core temperature estimation from heart rate time-series data, while Pham et al. (2020) developed a mobile health platform integrating multiple physiological and activity metrics. Hakim et al. (2025) further reviewed industry-focused studies using multi-sensor monitoring systems that combine physiological and environmental measurements. Despite these advances, real-time sensor-based monitoring across large and mobile construction workforces remains challenging due to technical skill requirements, cost, logistics, sensor reliability, and complex data processing (Ojha et al., 2024; Yan et al., 2022).

In response, predictive models can estimate human physiological responses under HS, providing a feasible way for simulating and assessing individual HS in occupational settings. Particularly, the MN-FTM and TN-TPM simplify the human body into core and skin compartments (Gagge 1971; Gagge et al. 1986; Fiala et al., 1999) for assessing thermoregulatory performances. It can simulate metabolic heat production, conductive heat transfer from core to skin, heat exchange with the environment via convection and radiation, and evaporative heat loss through sweating. This approach captures dynamic interactions between physiological and environmental variables while remaining computationally efficient, making it suitable for hourly prediction in field conditions. Empirical regression-based models can further complement this approach by linking HR to metabolic rate, body surface area, environmental factors, and individual characteristics, allowing estimation of cardiovascular strain without continuous physiological measurements. Accordingly, MN-FTM and TN-TPM are well-positioned for deployment in construction contexts, where dynamic site conditions and limited real-time data necessitate fast, reliable insights to support safety and operational decisions.

However, there is limited evidence demonstrating the application of integrated HS simulation and estimation frameworks that combine mechanistic modeling with realistic meteorological and worker-specific inputs (Yermakova et al., 2022). Hence, a critical gap remains between existing HS assessment methods and the operational needs of construction safety management. Construction sites involve variable task demands, heterogeneous microclimates, and limited feasibility for continuous physiological monitoring, reducing the effectiveness of both generalized heat indices and sensor-based approaches. Construction practitioners, therefore, need scalable and computationally efficient tools that estimate worker-specific thermo-physiological responses using readily available meteorological and task-related data. Yet, few modeling approaches are structured to directly support

construction decision-making, such as identifying high-risk exposure periods, informing work–rest scheduling, or prioritizing protective interventions for vulnerable workers.
To address this gap, this study aims to: (1) simulate and predict T_{core}, T_{skin}, and HR using an integrated thermophysiological framework; (2) evaluate relationships between physiological responses and environmental heat indices; and (3) identify critical exposure periods and vulnerable worker groups for actionable work–rest scheduling. Simulations use hourly summer meteorological data from Sacramento County, California, and representative worker characteristics from the literature. By providing scalable and practical heat strain estimates, this integrated modeling framework facilitates informed work-rest scheduling and targeted risk management to mitigate HRIs and productivity loss in outdoor construction.

Materials and Methodology

Study Area and Data Source

The study considered the greater Sacramento County region of California, encompassing six counties across an area of approximately 32,000 km² (Taha, 2021). Sacramento features a Mediterranean climate with hot-dry summers and mild-wet winters. Summer temperatures often exceed 40°C, with prolonged heat waves posing significant health risks for outdoor workers (Kwan et al., 2004). Therefore, predicting the physiological status of workers during tasks performed in hot weather, particularly throughout the summer season, is crucial for ensuring their health, safety, and productivity. Ranges of construction workers' age, height, weight, and activity level were obtained from published studies (Fletcher et al., 2020; Sammito et al., 2024; Yi & Chan, 2016) and used to create six representative worker cases without collecting new individual data. Moreover, hourly weather parameters, including air temperature (T_{air}), wind speed (V_a), relative humidity (RH), and solar radiation (R_s) from the Buffalo Creek Station, managed by the California Air Resources Board. The physiological parameters were then simulated and computed using MATLAB R2025a (The MathWorks, Natick, MA, USA) within the predictive, simulation-based framework. The day has been chosen from the summer months in 2024 (July and August) in terms of the highest temperature observed. Mean radiant temperature (T_{mrt}) was calculated using T_{air} and R_s according to eq. (1).

$$\mathrm{T_{mrt}} = \mathrm{T_{air}} + 0.0145\mathrm{R_s} \dots\dots\dots\dots\dots\dots (1)$$

Core and Skin Temperature

Metabolic rate (MR) refers to the amount of energy expended by the body to maintain essential physiological functions, which varies with gender, age, and obesity status, with men having higher rates than women (Butte et al., 2003). Resting Metabolic Rate (MR_{rest}), also called resting energy expenditure, accounts for the largest portion of total daily energy needs (Astrup et al., 1999). It is defined as the energy required by the body in a resting, awake, postabsorptive, and thermoneutral state (Bray, 2014), which can be calculated by following eq. (2).

$$\mathrm{MR_{rest}} = \frac{10 \times \mathrm{W} + 6.25 \times \mathrm{H} - 5 \times \mathrm{Ag} + 5}{\mathrm{A_D}} \times 0.0484 \dots\dots\dots\dots\dots\dots\dots (2)$$

According to a previous study (Du BOIS, 1916), human body area (A_D) depends on body height (H) and weight (W), which can be calculated by the following eq. (3).

$$\mathrm{A_D} = 0.20247 \times \mathrm{H}^{0.725} \times \mathrm{W}^{0.425} \dots\dots\dots\dots\dots..(3)$$

The working MR or MR_{work} varies according to the intensity and physical effort required to perform specific tasks. On construction sites, different occupations, such as bricklayers, scaffolders, carpenters, plumbers, and painters, are associated with varying levels of physical exertion, where heavier activities demand higher MR values (Hartmann & Fleischer, 2005). In this study, four representative MR levels were selected to reflect typical construction activities, while three MR_{work} values were used to capture task-specific variations. A value of zero was assigned during resting periods (MR_{rest}). The total metabolic rate (MR_T) was calculated by summing the resting and task-related metabolic rates, and the final MR_{work} was calculated following eq. (4) and (5).

$$\mathrm{MR_{work}} = \begin{cases} 0, & \text{resting periods} \\ 100;\ 200;\ 300, & \text{working periods (different works)} \end{cases} \quad \ldots\ldots\ldots\ldots..(4)$$

$$\mathrm{MR_T} = \mathrm{MR_{rest}} + \mathrm{MR_{work}} \ldots\ldots\ldots\ldots\ldots\ldots\ldots\ldots\ldots\ldots\ldots\ldots..(5)$$

A modified empirical formulation, adapted from the MN-FTM (Fiala et al., 1999), is presented in eq. (6), which predicts the dynamic response of human T_{core} to variations in MR, T_{mrt}, and V_a. On the other hand, T_{skin} is predicted by Gagge's TN-TPM (Gagge, 1971), as shown in eq. (7).

$$\mathrm{T_{core}} = 36.6 + 0.0025 \times (\mathrm{MR_T} - 80) + 0.01 \times (\mathrm{T_{mrt}} - 30) - 0.001 \times (\mathrm{V_a} - 0.3) \ldots\ldots..(6)$$

$$\mathrm{T_{skin}} = 33.5 + 0.01 \times (\mathrm{T_{air}} - 25) + 0.005 \times (\mathrm{T_{mrt}} - 30) - 0.2 \times \log(\mathrm{V_a} + 0.5) \ldots\ldots\ldots\ldots...(7)$$

The coefficients in these equations were empirically derived in previous studies through regression fitting to outputs from full multi-node physiological simulations under controlled environmental and metabolic conditions.

Heart Rate

The HR of construction workers was estimated considering both metabolic workload and thermal stress. The methodology builds upon the conventional HR prediction model (Yokota et al., 2008) and incorporates a temperature-dependent thermal stress factor. The thermal stress factor (S_f) was modeled as a fractional increase in HR per degree Celsius above a comfort threshold (25°C) according to ISO (1999) by the following eq. (8).

$$\mathrm{S_f} = \begin{cases} 0.15 \times (\mathrm{T_{air}} - 25), & \mathrm{T_{air}} > 25\ °\mathrm{C} \\ 0, & \mathrm{T_{air}} \leq 25\ °\mathrm{C} \end{cases} \quad \ldots\ldots\ldots\ldots\ldots\ldots\ldots.(8)$$

Here, T_{air} is the ambient air temperature in °C. The predicted HR considering metabolic rate (MR, W/m²) and thermal stress was then calculated using a modified Yokota-like model following eq. (9).

$$\mathrm{HR} = \max\left[\mathrm{HR_{rest}}, \min\left(\mathrm{HR_{rest}}(1 + 0.1\mathrm{S_f})\ \mathrm{HR_{rest}} \times \left(1 - \frac{\mathrm{MR} - \mathrm{C}}{\mathrm{K}}\right) \times (1 + \mathrm{S_f})\right)\right] \ldots\ldots(9)$$

Here, HR_{rest} and MR are the resting HR and metabolic rate, respectively, and C and K are empirical constants that were taken from prior modeling studies that relate metabolic rate and thermal strain to cardiovascular response. These coefficients represent generalized physiological responses and are intended for scenario-based prediction rather than subject-specific calibration.

Results

This study classified six representative cases (Case 1- Case 6) based on variations in age, height, weight, and MR, as detailed in Table 1. The cases were designed to cover a range of worker characteristics as independent strata, without implying any correlation between these variables. For each case, the T_{core}, $T_{skin,}$ and HR were computed over 24 hours. Three distinct MR were considered to represent different work intensities: 200 W/m² for Cases 1 and 2, 300 W/m² for Cases 3 and 4, and 100 W/m² for Cases 5 and 6, assigned in a randomized manner.

Table 1. Different cases representing various ranges of age, weight, height, and MR

Case	Age (years)	Resting HR (bpm)	Weight (kg)	Height (cm)	MR(W/m^2)
1	20-30	58-68	50-60	140-153	200
2	30-40	60-70	60-70	153-166	
3	40-50	62-72	70-80	166-179	300
4	50-60	64-74	80-90	179-192	
5	60-70	66-76	90-100	192-205	100
6	70-80	68-78	100-110	205-218	

The diurnal variation of the predicted T_{core}, T_{air}, and thermal load index (TLI) for outdoor construction workers under typical summer conditions is illustrated in Figure 1. The 3D surface plot (left) reveals that T_{core} remained stable (36.5-37.2 °C) during early morning and late evening but rose sharply between 7:00 AM and 12:00 PM, coinciding with peak solar radiation and elevated T_{air}. Both the TLI and $\Delta(T_{core} - T_{skin})$ (difference between T_{core} and T_{skin}) showed a sharp rise during the morning hours (right panel), coinciding with the start of the work shift and highlighting the critical exposure zone for outdoor workers.

TLI and $\Delta(T_{core} - T_{skin})$ peaked at approximately 340 and 5.2 °C, respectively, indicating intensified metabolic activity and a strong temperature gradient between the body core and skin. After this point, $\Delta(T_{core} - T_{skin})$ declined steadily while TLI continued to increase, suggesting that the body accumulated heat faster than it could dissipate it through the skin. Both parameters stabilized around 6:00 PM before showing minor fluctuations with evening cooling, reflecting partial thermal recovery.

Three-dimensional regression surface of T_{skin} as a function of T_{air} and T_{mrt} is illustrated in Figure 2. The fitted plane demonstrates a clear linear dependence, where T_{skin} increases with both T_{air} and T_{mrt}, indicating a strong coupling between convective and radiative heat exchanges. The regression surface captures the thermal interaction effectively, with the color gradient emphasizing regions of higher predicted T_{skin} approaching 39 °C under combined high T_{air} and T_{mrt} conditions.

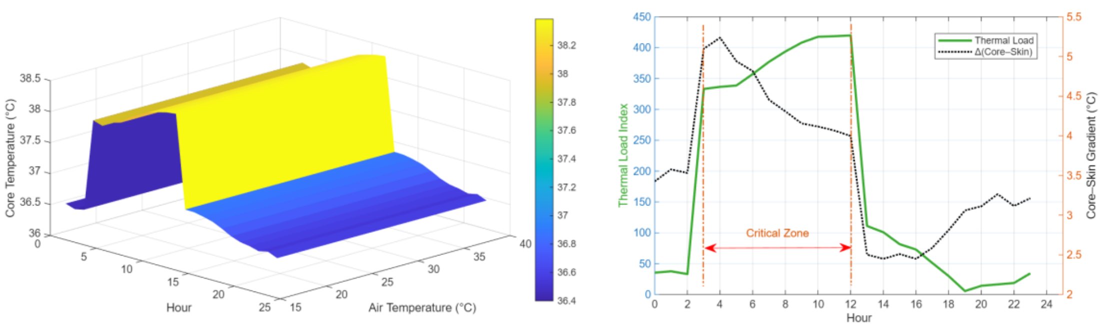

Figure 1. Simulated 24-hour pattern of core temperature and thermal load response under typical summer conditions

The close alignment of measured data points (black markers) with the regression plane indicates minimal residual variation and supports the reliability of the model. The findings align with the human thermophysiological behavior reported by Parsons (2007) and Gagge et al. (1986), where both convective components significantly influence peripheral skin temperature. Similar response magnitudes were observed in controlled laboratory studies, where each 1°C increase in T_{air} raised T_{skin} by 0.10-0.15°C under moderate metabolic activity (Standardization, 2004).

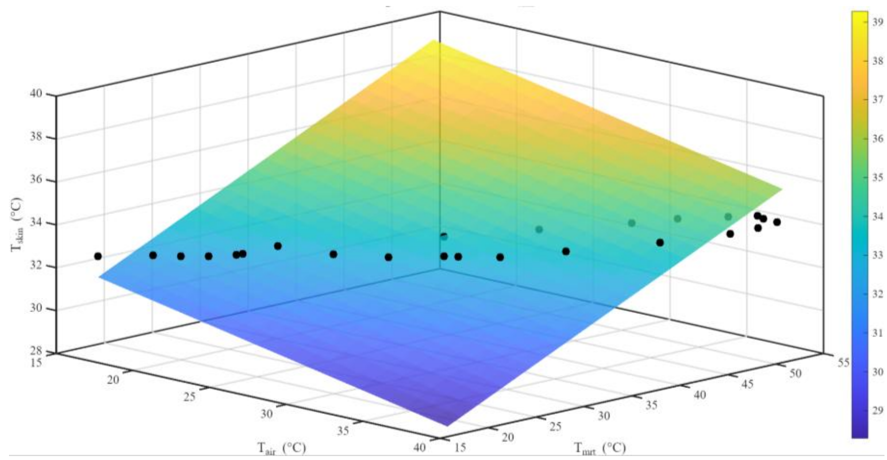

Figure 2. 3D regression surface of predicted T_{skin} as a function of T_{air} and T_{mrt}

The relations of T_{core} and HR with different cases are highlighted in Figure 3. HR exhibited a significant decreasing trend (2nd degree with $R^2 = 0.92$), dropping from about 165 bpm in Case-1 to approximately 145 bpm in Case-6. This decline suggests a gradual cardiovascular adjustment as both body morphology and heat exposure conditions changed, indicating improved thermoregulatory stability among workers with higher body height and mass and lower radiant load. Conversely, T_{core} displayed a moderate nonlinear trend ($R^2 = 0.67$), increasing from 37°C in Case-1 to a peak of 37.2°C at Case-3 before declining to 36.8°C by Case-6. The mid-scenario elevation corresponds to the 300 W/m² exposure, highlighting enhanced metabolic and thermal load, while the later decline reflects reduced heat flux and compensatory evaporative cooling (Fiala et al., 2012). The contrasting trends between HR and T_{core} emphasize the nonlinear and time-dependent nature of human thermoregulation.

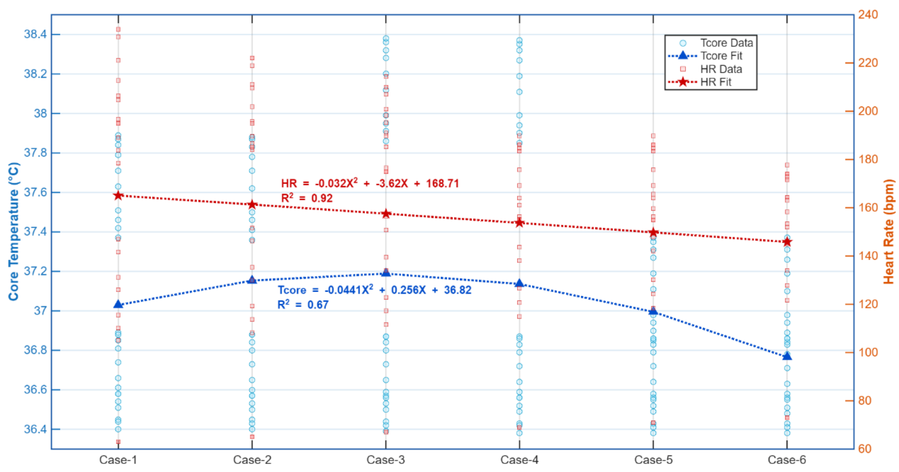

Figure 3. Relationship between predicted core temperature and heart rate under varying anthropometric and heat exposure conditions

The diurnal profiles of T_{core} and HR for six representative cases, where data were smoothed and presented with ±1 standard deviation (SD) to highlight temporal variability across cases illustrated in Figure 4. In all scenarios, T_{core} shows a pronounced rise from early morning (≈36.5-38 °C at 06:00 h) to late morning (peak ≈37.5-38.5 °C around 10:00-12:00 h), followed by a gradual decline toward evening. The increase reflects the combined influence of metabolic heat production and progressive solar load during mid-day hours. Similarly, HR exhibits a diurnal pattern, rising from ~95 bpm during early rest periods to peak values of 180-220 bpm during the late-morning to mid-day period, particularly in Cases 3 and 4, indicating elevated MR (300 W/m^2) strain under intense thermal conditions. Although younger and lighter workers exhibited higher peak HR during maximum thermal stress, their HR declined sharply during the late afternoon rest period. In contrast, older and heavier workers experienced comparatively lower peak values but maintained elevated HR levels even after work cessation, indicating delayed cardiovascular recovery and prolonged thermal strain. After 16:00 h, both T_{core} and HR progressively decline as environmental temperature and metabolic demands decrease. The synchronization between T_{core} and HR patterns illustrated a strong thermophysiological coupling, consistent with human heat-balance mechanisms where elevated MR accelerates cardiovascular output to facilitate skin blood flow and heat dissipation (Parsons, 2007).

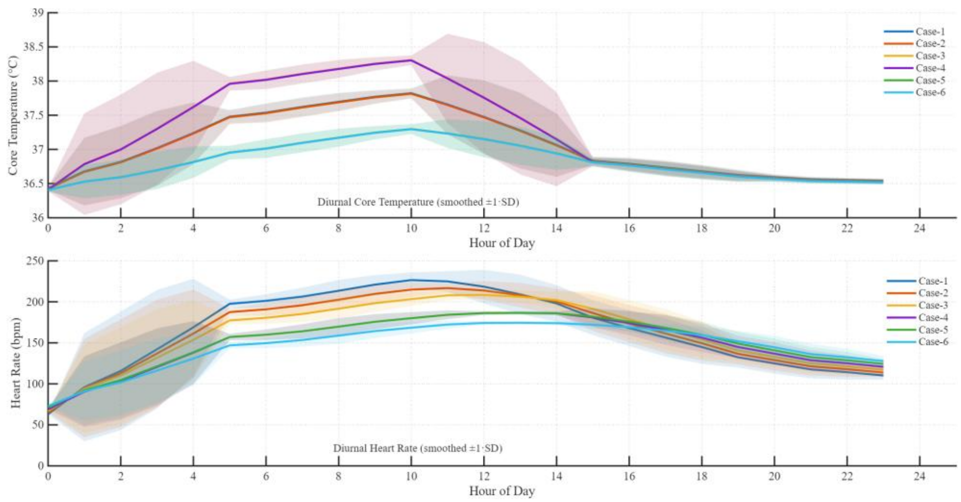

Figure 4. Diurnal variation of T_{core} and HR for six representative cases, showing mean values with ±1 SD under varying thermal exposure conditions

Figure 5 illustrates the diurnal distribution of percentage heart rate exceedance (%HR Exceeds) for six representative cases, reflecting variations in thermal load and metabolic intensity across a 24-hour work cycle.

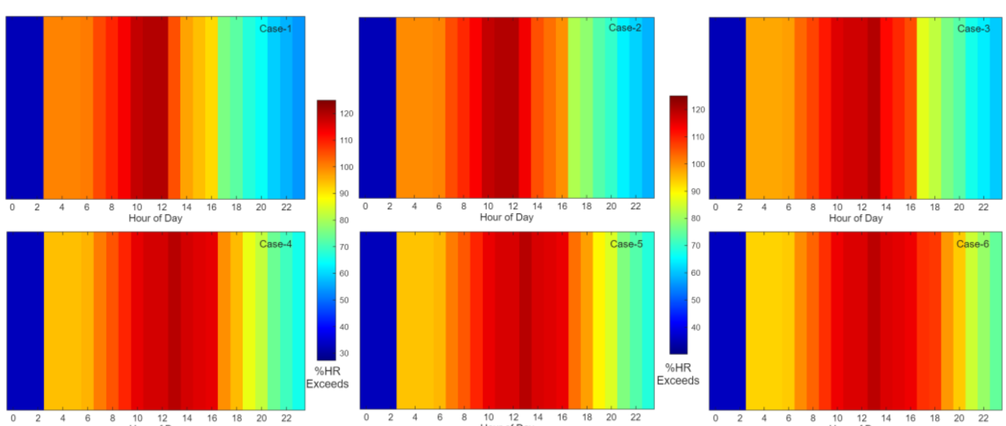

Figure 5. Comparison of diurnal heart rate exceedance (%HR Exceeds) among six worker cases

A distinct temporal trend was observed, with HR exceedance values remaining relatively low during early morning (0:00-6:00 h), followed by a sharp escalation during the mid-day period (10:00-15:00 h), coinciding with peak T_{air} and radiant heat exposure. The intensity of cardiovascular strain varied across cases, with Cases 3 and 4 (300 W/m^2) showing the highest HR exceedance levels exceeding 120% of baseline, indicating conditions of severe thermal stress and elevated cardiovascular workload. In contrast, Cases 1 and 2 (200 W/m^2) showed moderate HR responses (90-110%), while Cases 5 and 6 (100 W/m^2) remained mostly below 80%, suggesting acceptable physiological adaptation under lower MR. The diurnal trend highlights that mid-day hours represent a critical window of elevated physiological stress, during which thermal load surpasses the body's compensatory mechanisms, triggering accelerated heart rate to support convective heat dissipation and peripheral blood flow redistribution (Sessler, 1993).

Discussion

This study shows that predictive thermo-physiological modeling can assess construction workers' heat strain when real-time monitoring is impractical. The rapid rise in predicted T_{core} toward ~38.2 °C signals the onset of moderate to severe heat strain, consistent with ISO 9886 tolerance limits (Standardization, 2004) and established links to impaired thermoregulation and elevated risks of fatigue, dehydration, and heat-related illness (Parsons, 2003). Peak physiological strain between 11:00 AM and 1:00 PM aligns with previous field evidence of maximum cardiovascular and thermal stress during late morning to early afternoon under hot-humid conditions (Acharya et al., 2018), supporting the realism of the simulations. Notably, HR responded more rapidly to external heat and metabolic demand, whereas T_{core} exhibited a delayed increase due to cumulative heat storage, consistent with thermophysiological theory (Kim & Lockhart, 2008) and prior field findings identifying HR as an early indicator of acute strain and T_{core} as a marker of sustained thermal load (Factor, 2014). The observed nonlinear (second-order) relationships between heat exposure, HR, and T_{core} highlight the limitations of simplified empirical approaches in representing physiological responses under extreme heat. By integrating multi-node and two-node thermophysiological models with heart-rate estimation, this study bridges the gap between controlled research and field-ready heat stress management, offering a scalable and actionable framework that accounts for environmental, workload, and individual variability.

From an applied perspective, the findings provide clear implications for construction heat risk management. To complement continuous physiological monitoring or daily individualized measurements, the proposed framework functions as a scenario-based decision-support tool that integrates readily available meteorological data and different representative worker groups with different characteristics. This enables practitioners to identify critical exposure periods, anticipate elevated risk among vulnerable groups (e.g., workers with higher metabolic rates), and optimize work-rest scheduling during peak thermal load periods. Such an approach directly addresses the operational constraints highlighted in prior studies concerning the feasibility of large-scale wearable monitoring in dynamic construction settings (Rane et al., 2023). To capture broad parameter variability, this study analyzed six representative cases varying in age, height, weight, and MR. While these factors are often interconnected in complex ways, they were treated as independent variables to simplify the framework. This approach remains scalable and can be applied to any worker combination beyond the initial cases studied.

Conclusions

Worker safety and performance in extreme thermal conditions largely depend on physiological responses, including HR, T_{core}, and T_{skin}, which are challenging to measure of large workforce directly in the field. This study presents a simulation-based framework to predict these parameters using a modified MN-FTM alongside a conventional prediction model (i.e., TN-TPM) incorporating meteorological data and individual characteristics. Six scenarios were simulated based on combinations of age, weight, height, and three MRs. Results indicate that T_{skin} varied linearly with T_{air} and T_{mrt} throughout the day, whereas T_{core} peaked around 38 °C at midday. The largest $\Delta(T_{core} - T_{skin})$ occurred at 10 AM, shortly after work commenced. HR exhibited a pronounced second-order declining trend ($HR = -0.032X^2 – 3.62X + 168.71$; $R^2 = 0.92$), while T_{core} followed a moderate parabolic pattern ($T_{core} = -0.0441X^2 + 0.256X + 36.82$; $R^2 = 0.67$), reflecting nonlinear thermo-physiological adaptations under varying worker characteristics and MR. Younger and lighter workers experienced higher peak HR under maximum HS but recovered rapidly during rest, whereas older, heavier workers showed lower peaks yet maintained elevated HR levels after work cessation. The study relies on predictive models rather than continuous field data and considers limited combinations of age, height, weight, and metabolic rate, while excluding factors such as gender, hydration, clothing, and rapid environmental changes. Accordingly, the results should be interpreted as scenario-based predictions under controlled, idealized conditions. Future work should focus on field validation, expanding worker profiles and environmental variability, and developing real-time predictive tools to enhance model accuracy and support adaptive, climate-resilient work practices.

References

Acharya, P., Boggess, B., & Zhang, K. (2018). Assessing Heat Stress and Health among Construction Workers in a Changing Climate: A Review. *International Journal of Environmental Research and Public Health*, *15*(2), 247. https://doi.org/10.3390/ijerph15020247

Astrup, A., Gøtzsche, P. C., van de Werken, K., Ranneries, C., Toubro, S., Raben, A., & Buemann, B. (1999). Meta-analysis of resting metabolic rate in formerly obese subjects. *The American Journal of Clinical Nutrition*, *69*(6), 1117–1122. https://doi.org/10.1093/ajcn/69.6.1117

Bray, G. A. (2014). *Handbook of Obesity--Volume 1: Epidemiology, Etiology, and Physiopathology* (Vol. 1). CRC Press.

Buller, M. J., Welles, A. P., & Friedl, K. E. (2018). Wearable physiological monitoring for human thermal-work strain optimization. *Journal of Applied Physiology*, *124*(2), 432–441. https://doi.org/10.1152/japplphysiol.00353.2017

Butte, N. F., Treuth, M. S., Mehta, N. R., Wong, W. W., Hopkinson, J. M., & Smith, E. O. (2003). Energy requirements of women of reproductive age. *The American Journal of Clinical Nutrition*, *77*(3), 630–638. https://doi.org/10.1093/ajcn/77.3.630

Du BOIS, D. (1916). CLINICAL CALORIMETRY. *Archives of Internal Medicine*, *XVII*(6_2), 863. https://doi.org/10.1001/archinte.1916.00080130010002

Factor, R. (2014). The effect of traffic tickets on road traffic crashes. *Accident Analysis & Prevention*, *64*, 86–91. https://doi.org/10.1016/j.aap.2013.11.010

Fiala, D., Havenith, G., Bröde, P., Kampmann, B., & Jendritzky, G. (2012). UTCI-Fiala multi-node model of human heat transfer and temperature regulation. *International Journal of Biometeorology*, *56*(3), 429–441. https://doi.org/10.1007/s00484-011-0424-7

Fiala, D., Lomas, K. J., & Stohrer, M. (1999). A computer model of human thermoregulation for a wide range of environmental conditions: the passive system. *Journal of Applied Physiology*, *87*(5), 1957–1972. https://doi.org/10.1152/jappl.1999.87.5.1957

Fletcher, M. J., Glew, D. W., Hardy, A., & Gorse, C. (2020). A modified approach to metabolic rate determination for thermal comfort prediction during high metabolic rate activities. *Building and Environment*, *185*, 107302. https://doi.org/10.1016/j.buildenv.2020.107302

Gagge, A. P. (1971). An effective temperature scale based on a simple model of human physiological regulatory response. *Ashrae Trans.*, *77*, 247–262.

Gagge, A. P., Fobelets, A. P., & Berglund, L. (1986). *A standard predictive index of human response to the thermal environment.*

Hakim, I. N., Utami, S. S., Lestari, T., & Norpiadi, N. (2025). *A Review on Health Monitoring System for Industry Workers: Requirement, System, and Performance*. 256–272. https://doi.org/10.4028/p-6epWVk

Hartmann, B., & Fleischer, A. G. (2005). Physical load exposure at construction sites. *Scandinavian Journal of Work, Environment & Health*, 88–95.

International standards for the assessment of the risk of thermal strain on clothed workers in hot environments. (1999). *The Annals of Occupational Hygiene*. https://doi.org/10.1093/annhyg/43.5.297

KIM, S., & LOCKHART, T. E. (2008). The Effects of 10% Front Load Carriage on the Likelihood of Slips and Falls. *Industrial Health*, *46*(1), 32–39. https://doi.org/10.2486/indhealth.46.32

Kwan, M., Woo, J., & Kwok, T. (2004). The standard oxygen consumption value equivalent to one metabolic equivalent (3.5 ml/min/kg) is not appropriate for elderly people. *International Journal of Food Sciences and Nutrition*, *55*(3), 179–182. https://doi.org/10.1080/09637480410001725201

Parsons, K. (2003). The effects of hot, moderate, and cold environments on human health, comfort and performance. *Human Thermal Environments. London: Taylor & Francis*.

Parsons, K. (2007). *Human Thermal Environments*. CRC Press. https://doi.org/10.1201/9781420025248

Pham, S., Yeap, D., Escalera, G., Basu, R., Wu, X., Kenyon, N. J., Hertz-Picciotto, I., Ko, M. J., & Davis, C. E. (2020). Wearable Sensor System to Monitor Physical Activity and the Physiological Effects of Heat Exposure. *Sensors*, *20*(3), 855. https://doi.org/10.3390/s20030855

Rane, N., Choudhary, S., & Rane, J. (2023). Leading-edge wearable technologies in enhancing personalized safety on construction sites: a review. *SSRN Electronic Journal*. https://doi.org/10.2139/ssrn.4641480

Sammito, S., Thielmann, B., Klussmann, A., Deußen, A., Braumann, K.-M., & Böckelmann, I. (2024). Guideline for the application of heart rate and heart rate variability in occupational medicine and occupational health science. *Journal of Occupational Medicine and Toxicology*, *19*(1), 15. https://doi.org/10.1186/s12995-024-00414-9

Sessler, D. I. (1993). Perianesthetic thermoregulation and heat balance in humans. *The FASEB Journal*, *7*(8), 638–644. https://doi.org/10.1096/fasebj.7.8.8500688

Standardization, I. O. for. (2004). *Ergonomics-Evaluation of thermal strain by physiological measurements*. International Organization for Standardization.

Taha, H. (2021). Development of an Urban Heat Mitigation Plan for the Greater Sacramento Valley, California, a Csa Koppen Climate Type. *Sustainability*, *13*(17), 9709. https://doi.org/10.3390/su13179709

Yi, W., & Chan, A. (2016). Health Profile of Construction Workers in Hong Kong. *International Journal of Environmental Research and Public Health*, *13*(12), 1232. https://doi.org/10.3390/ijerph13121232

Yokota, M., Berglund, L., Cheuvront, S., Santee, W., Latzka, W., Montain, S., Kolka, M., & Moran, D. (2008). Thermoregulatory model to predict physiological status from ambient environment and heart rate. *Computers in Biology and Medicine*, *38*(11–12), 1187–1193. https://doi.org/10.1016/j.compbiomed.2008.09.003